1   **Dispersal in dendritic networks: ecological consequences on**

2   **the spatial distribution of population densities**

3

4   Florian Altermatt[1,2,*] & Emanuel A. Fronhofer[1,2]

5

6   [1] Eawag, Swiss Federal Institute of Aquatic Science and Technology, Department of

7   Aquatic Ecology, Überlandstrasse 133, CH-8600 Dübendorf, Switzerland.

8   [2] Department of Evolutionary Biology and Environmental Studies, University of

9   Zurich, Winterthurerstr. 190, CH-8057 Zürich, Switzerland.

10

11   *corresponding author: Florian.Altermatt@eawag.ch

12

13

14   **Number of words:** 7700

15   **Number of figures:** 6

16   **Number of tables:** 4

17

18   **Abstract**

19   1. Understanding the consequences of spatial structure on ecological dynamics is a

20   central theme in ecology. Recently, research has recognized the relevance of river and

21   river-analogue network structures, because these systems are not only highly diverse

22   but also rapidly changing due to habitat modifications or species invasions.

23   2. Much of the previous work on ecological and evolutionary dynamics in

24   metapopulations and metacommunities in dendritic river networks has been either

25   using comparative approaches or was purely theoretical. However, the use of

26   microcosm experiments provides the unique opportunity to study large-scale questions

27   in a causal and experimental framework.

28   2. We conducted replicated microcosm experiments, in which we manipulated the

29   spatially explicit network configuration of a landscape and addressed how linear *versus*

30   dendritic connectivity affects population dynamics, specifically the spatial distribution

31   of population densities, and movement behavior of the protist model organism

32   *Tetrahymena pyriformis*. We tracked population densities and individual-level

33   movement behavior of thousands of individuals over time.

34   3. At the end of the experiment, we found more variable population densities between

35   patches in dendritic networks compared to linear networks, as predicted by theory.

36   Specifically, in dendritic networks, population densities were higher at nodes that

37   connected to headwaters compared to the headwaters themselves and to more central

38   nodes in the network. These differences follow theoretical predictions and emerged

39   from the different network topologies *per se*. These differences in population densities

40   emerged despite weakly density-dependent movement.

41   4. We show that differences in network structure alone can cause characteristic spatial

42   variation in population densities. While such differences have been postulated by

43   theoretical work and are the underlying precondition for differential dispersal evolution

44   in heterogeneous networks, our results may be the first experimental demonstration

45   thereof. Furthermore, these population-level dynamics may affect extinction risks and

46   can upscale to previously shown metacommunity level diversity dynamics. Given that

47   many species in natural river systems exhibit strong spatio-temporal patterns in

48   population densities, our work suggests that abundance patterns should not only be

49   addressed from a local environmental perspective, but may be the outcome of processes

50   that are inherently driven by the respective habitat network structure.

51

52   **Key words:** Dispersal, bacteria-protist metacommunities, microcosm experiment,

53   river-like networks, protists, ecological theory.

54

Introduction

An extensive part of classic theoretical and empirical ecology has focused on localized

and well-mixed populations or communities. However, in most natural systems,

populations and communities are heterogeneous and spatially structured with dispersal

connecting patches across space. The spatial structure and dynamics across multiple

populations or communities may strongly affect local dynamics, and the study of

spatial dynamics has more recently become a central theme in ecology (Hanski, 1999;

Leibold *et al.*, 2004).

        Spatial dynamics are likely relevant and occurring in all ecosystems and habitat

types, but may be especially prevalent in some ecosystems due to specific intrinsic

geophysical structures. River networks may be the most prominent example thereof

(Grant, Lowe & Fagan, 2007; Brown & Swan, 2010; Altermatt, 2013; Peterson *et al.*,

2013). Rivers and river networks are shaped by very general geological processes

(Rodriguez-Iturbe & Rinaldo, 1997), which result in characteristic and universal spatial

network structures. The significance of spatial dynamics in these fractal, dendritic

networks has received much interest over the last years (e.g., Grant, Lowe & Fagan,

2007; Muneepeerakul *et al.*, 2008; Carrara *et al.*, 2012; Peterson *et al.*, 2013; Mari *et*

al., 2014; Seymour, Fronhofer & Altermatt, 2015) due to the universality of the spatial

network, often defining dispersal pathways, and due to the exceptionally high diversity

found in natural river systems (Dudgeon *et al.*, 2006; Vorosmarty *et al.*, 2010).

Furthermore, in many natural river systems both the network structure and the

biological communities are currently rapidly changing due to habitat modifications,

building of dams across waterways or species invasions (Vorosmarty *et al.*, 2010;

Lynch *et al.*, 2011). This creates an immediate need for a better understanding of how

river and river-analogue network structures drive population and community dynamics.

80   Extensive previous work addressing ecological and evolutionary dynamics in

81   dendritic river networks has been either using comparative approaches or was purely

82   theoretical. Empirical studies have for example documented that local habitat

83   conditions and network position affect the composition of local communities and

84   abundances of organisms (e.g., Heino, Muotka & Paavola, 2003; Altermatt, Seymour

85   & Martinez, 2013; Liu *et al.*, 2013; Tonkin, 2014; Heino *et al.*, 2015). Theoretical

86   studies have been extensively addressing how network structure and dispersal along the

87   specific network configuration drive metacommunity composition and biodiversity

88   (e.g., Muneepeerakul *et al.*, 2008; Fagan *et al.*, 2009; Peterson *et al.*, 2013; Mari *et*

89   *al.*, 2014). More recently, models have incorporated eco-evolutionary dynamics and

90   feedbacks to investigate if and how river-like network structures are more likely to

91   result in fluctuations of population densities and subsequent classic metapopulation

92   dynamics compared to linear landscapes or other types of networks (Fronhofer &

93   Altermatt, 2017). Such population-level fluctuations may eventually affect extinction

94   dynamics and are thereby the underlying process shaping (meta)community structure

95   and diversity. While both comparative and theoretical approaches are highly important,

96   we currently lack a causal experimental breakdown of local *versus* regional factors

97   driving the observed population dynamics. Microcosm experiments may fill this gap, as

98   they offer a possibility to bridge from theoretical models to comparative field studies.

99   Microcosm experiments have a long tradition in ecology, and have been

100   important in improving our understanding of predator-prey dynamics (Gause, 1934;

101   Holyoak & Lawler, 1996; Hiltunen, Ayan & Becks, 2015), competitive interactions

102   (Cadotte *et al.*, 2006; Livingston *et al.*, 2012; Carrara *et al.*, 2015), dispersal ecology

103   (e.g., Cadotte *et al.*, 2006; Jacob *et al.*, 2015), or evolutionary dynamics (Bell &

104   Gonzalez, 2009; Hiltunen & Becks, 2014; Fronhofer & Altermatt, 2015; Van

105   Petegem *et al.*, 2016). The goal of these studies is not to give a 1:1 representation of a

106   real ecosystem, but rather to disentangle individual driving factors in a causal approach,

107   and to give empirical proof of principles of theoretically postulated processes (Jessup *et*

108   *al.*, 2004; Altermatt *et al.*, 2015). Such microcosm experiments are thought to be

109   especially advantageous in addressing questions that include otherwise (i.e., in the

110   natural system) large spatial or temporal scales. It is thus of no surprise that microcosm

111   experiments have recently been extensively used to address the significance of spatial

112   dynamics on community composition and biodiversity in riverine ecosystems. Many of

113   these studies have been giving insights into how dispersal in dendritic network

114   structures gives rise to characteristic diversity patterns (Carrara *et al.*, 2012; Carrara *et*

115   *al.*, 2014; Seymour & Altermatt, 2014; Seymour, Fronhofer & Altermatt, 2015). The

116   focus of all of these studies was at the metacommunity level and they were looking at

117   integrative measures of biodiversity (usually number of species/α-diversity). Thereby

118   they largely neglected the underlying distributions and dynamics of population

119   densities in the networks. Importantly, the combination of all these population level

120   demographic processes will eventually shape metacommunity composition and

121   structure. Yet, such population dynamics in single species systems have hitherto only

122   been studied in an invasion context in linear landscapes (Giometto *et al.*, 2014;

123   Fronhofer & Altermatt, 2015; Fronhofer, Nitsche & Altermatt, 2017; Giometto,

124   Altermatt & Rinaldo, 2017).

125   Population level dynamics, however, are critical for population viability,

126   conservation and evolutionary dynamics. For example, recent theoretical work shows

127   that heterogeneity in spatial connectivity is a crucial component for the evolution of

128   dispersal (Henriques-Silva *et al.*, 2015), which directly affects (meta)population level

129   metrics such as indices of genetic population differentiations and extinction likelihoods

130   (Fronhofer & Altermatt, 2017), and eventually also metacommunity composition. An

131   underlying theoretical component of all these dynamics is a dependency of population

132   sizes on network connectivity. To our knowledge, however, there is hitherto no

133   experimental work that has assessed the effect of spatial network configurations on

134   population density distributions and dynamics.

135   We used protist microcosm experiments to study the effect of spatial network

136   configuration, specifically linear *versus* dendritic connectivity, on population dynamics

137   and movement behavior of the ciliate model organism *Tetrahymena pyriformis* kept on

138   a bacterial resource. Using replicated multi-patch landscapes of different network

139   configuration (Fig. 1), we could assess abundance dynamics and movement behavior of

140   thousands of organisms over time. We show that differences in network structure alone

141   can cause characteristic spatial variation in population densities, as predicted by simple

142   theoretical considerations (Tab. 1). Our results suggest that the commonly observed

143   strong spatio-temporal fluctuations in population densities, and eventually

144   metacommunity structure, of many riverine organisms may not only be driven by local

145   dynamics, but may be the outcome of processes that are inherently linked to the habitat

146   network structure.

147

148   **Methods**

149   *Study system*

150   We use single-species protist microcosms to address the effect of spatial network

151   structure on population dynamics and density patterns across space and time. Such

152   protist microcosm experiments have a long history in ecology and evolution (Gause,

153   1934; Altermatt *et al.*, 2015), and allow to causally disentangle drivers of ecological

154   and/or evolutionary dynamics (e.g., Fjerdingstad *et al.*, 2007; Giometto *et al.*, 2014;

155   Fronhofer & Altermatt, 2015).

156   For our experiments we used the bacterivorous ciliate species *Tetrahymena*

157   *pyriformis* as a model organism. It has a body length and body volume of about 35 μm

158   and 1400 μm^3 respectively (Giometto *et al.*, 2013), high growth rates ($2 < r_0 < 4$ per day)

159   and equilibrium densities ($6{,}000 < K < 15{,}000$ per mL) (Fronhofer, Kropf & Altermatt,

160   2015), making it an ideal study organism to address population dynamics over short

161   time periods including many generations. All experiments were conducted using a

162   standard protist-culturing medium made from protist pellets (0.46 gL^{-1}; Carolina

163   Biological Supply) and inoculated with three different species of freshwater bacteria

164   (*Serratia fonticola, Bacillus subtilis* and *Brevibacillus brevis*). The nutrient medium

165   was autoclaved and inoculated with 5% of a dense, about 1-week old culture of these

166   bacteria. The protists (*Tetrahymena*) use these bacteria as resources. All organisms

167   used in the experiment are heterotrophic, but experiments were nevertheless conducted

168   under constant light at 20 °C to *a priori* avoid any photoperiodic effects (for further

169   details see Altermatt *et al.*, 2015). Importantly, the nutrient medium used in the

170   experiment was added at identical concentration to all patches at the onset of the

171   experiment, that is, all patches had strictly identical starting conditions and subsequent

172   differences cannot be attributed to initial differences. Abiotic resources (i.e., nutrients)

173   were not replenished subsequently during the experiment (contrary to chemostat

174   experiments). Thus, nutrients were depleted over the experiment by bacteria, which

175   themselves were fed on by *Tetrahymena*.

176

177   *Experimental design*

178   We constructed replicated linear and dendritic landscape networks of identical total

179   patch and landscape volume (i.e., regional habitat capacity) and total length of

180   connecting corridors, arranged according to the respective network structure (i.e., linear

181   *vs.* dendritic, Fig. 1; three replicated landscapes per network type). Networks were

182   constructed using 20 mL Sarstedt vials (Sarstedt, Nümbrecht, Germany), which were

183   connected with silicone tubes (silicone tube inner ø = 4 mm; VWR, Radnor, USA).

184   Stopcocks (Discofix, B. Braun, Sempach, Switzerland) allowed us to control dispersal.

185   The distance of each connecting tube including the stopcock was 6 cm. During all

186   handling and sampling of the landscapes, stopcocks were closed such that there was no

187   exchange of individuals due to the handling.

188   We filled the landscapes with 15 ml of medium, and inserted protists at

189   equilibrium density (approx. 1 week old cultures) at the onset of the experiment. We

190   then allowed dispersal of protists three times per week (Monday, Wednesday, Friday)

191   during 4 hours. This dispersal scenario was chosen based on extensive previous

192   knowledge (Fronhofer & Altermatt, 2015; Fronhofer, Nitsche & Altermatt, 2017),

193   showing that with a 4 h dispersal period we have dispersal rates of approximately 5 to

194   20 percent of the respective population. Thereby, population growth rates, intraspecific

195   competition and dispersal across the landscapes were interacting and driving population

196   dynamics and density distribution at the metapopulation scale. As all factors other than

197   network configuration (linear *vs.* dendritic) were kept constant, we can causally address

198   the effect of landscape networks structure on spatio-temporal population dynamics. All

199   60 microcosms were sampled at day 0, 8 and 15 of the experiment to assess protist

200   population densities and movement behavior.

201

202   *Data collection*

203   We assessed density as well as movement behavior of protists using microscopy

204   combined with automated video analysis using the free image analysis software

205   IMAGEJ (version 1.46a U. S. National Institutes of Health, Bethesda, MD, USA,

206   http://imagej.nih.gov/ij/) following the protocol by Pennekamp & Schtickzelle (2013).

207   Specifically, per sampling event, we sampled 0.5 mL of each population replicate, and

208   placed it in a counting cell chamber (total volume assessed per sample was 19 µL,

209   height of chamber 0.5 mm) under a Nikon SMZ1500 stereo-microscope (Nikon

210   Corporation, Kanagawa, Japan) at 30-fold magnification. Using a Hamamatsu Orca

211   Flash 4 video camera (Hamamatsu Photonics K.K., Hamamatsu city, Japan), we then

212   recorded 20 s videos (total of 500 frames) per sample. The scripted image analysis

213   determines in a first step the position of moving particles that fall into the size range of

214   20 to 200 pixels (correspond to the range of sizes these organisms can have, see also

215   Fronhofer, Kropf & Altermatt, 2015). This is done by subtracting information on

216   particles/pixels across all paired, subsequent frames per video, such that the difference

217   between two subsequent image frames can be extracted (i.e., one gets a "difference

218   image"). In a second step, the location of all these moving particles are relinked across

219   all frames to get movement paths of all protists in the video. This linking procedure

220   was done using the MOSAIC particle tracker plug-in (see also Fronhofer, Kropf &

221   Altermatt, 2015). Based on the output of these analyses, we extracted population sizes

222   (i.e., density) of protists as well as velocities, turning angle distribution, and net

223   distance travelled as our movement parameters for all individuals measured.

224

225   *Statistical analyses*

226   All analyses were done using R version 3.3.3 (R Development Core Team, 2016) and

227   data can be downloaded from Dryad (DOI: XXXX). We analyzed the data using linear

228   mixed effects models incorporated in the package *nlme* (version 3.1-131) (Pinheiro *et*

229   *al.*, 2016). We ranked all possible models of the respective fixed effects including

230   interactions based on the Akaike information criterion corrected for small sample sizes

231   (AICc) and assessed explanatory potential using AICc weights. For model selection we

232   used maximum likelihood (ML) estimates obtained by simulated annealing (optimizer

233   of lme function set to "optim" and "SANN") and the best fitting model was

234   subsequently refit using REML. For the density analyses we used square-root

235   transformed density data as the response variable. For the movement analyses we used

236   log-transformed Euclidean distances as the response variable. We included network

237   position (central *vs.* inner *vs.* outer nodes; see Fig. 1), network type (linear *vs.* dendritic)

238   and time (days 0, 8 and 15) as fixed effects. We also included time as a pseudo-

239   replicate within each landscape (unique landscape ID) as random effect, due to the

240   repeated measures of individual replicate microcosms over time.

241   The analysis of density-dependent movement included population density in a linear,

242   squared and cubed term as the relationship between movement, respectively dispersal,

243   and density is known to be non-linear in *T. pyriformis* (Fronhofer, Kropf & Altermatt,

244   2015). In this analysis "network" was also included as a fixed effect and the random

245   effect structure included "time" nested in "network" and "position".

246   As best models identified by the model selection procedure tended to have limited

247   support if one considered AICc weights (see, e.g., Tab. 2 and 4), we used full model

248   averaging (R package "MuMIn", version 1.15.6) to obtain a potentially less biased

249   model fits. Note that our conclusions are not affected by the specifics of our statistical

250   analysis, as the main effects we report can be found regardless of model averaging. In

251   order to keep the analyses of population densities and movement comparable, we used

252 population level means of the movement data, which leads to conservative analyses and

253 makes our findings more robust.

254 In order to compare variation in population densities between dendritic and linear

255 landscapes, we used the ratio between interquartile ranges (IQR) and medians of the

256 respective population densities. This measure is analogous to the coefficient of

257 variation, but more robust with regards to the distribution of the underlying data. We

258 analyzed the difference between IQR/median obtained from linear and dendritic

259 landscapes statistically using resampling (200,000 draws and random assignment to

260 either linear of dendritic) and a one-sided test, as the theoretical prediction is that

261 dendritic landscapes should exhibit higher variation in population densities than linear

262 landscapes (distribution reported in Fig. 4).

263

264 *Fitting theoretical expectations to data*

265 In order to fit the theoretical expectations summarized in Tab. 1 to the observed

266 population density data (only data from day 15) we used the Levenberg-Marquardt

267 nonlinear least-squares algorithm (R package "minpack.lm", version 1.2-1). The

268 function *nls.lm* minimizes the residuals between predicted and observed data. We

269 compared two approaches: 1) fitting the models assuming identical d and K values for

270 dendritic and linear landscapes and 2) allowing for landscape-specific d and K

271 estimates. These two models were compared using AICc. Population density estimates

272 were calculated using the fitted d and K values and the relationships shown in Tab. 1.

273 Confidence intervals were calculated using the standard error estimates provided by the

274 summary of the *nls.lm* function and appropriate error propagation using the R package

275 "propagate" (version 1.0-4).

276

277 **Results**

278 At the end of the experiment (day 15; Fig. 1), we observed differences in population

279 densities between networks and, for dendritic networks, also within the network

280 between different patch locations (central *vs*. inner *vs*. outer; Fig. 1 and 2). These

281 differences were captured quantitatively by the statistical models (Tab. 2). While the

282 full model showed the best fit (ΔAICc = 0), its support was somewhat ambiguous

283 (W_{AICc}=0.44). The fit of the averaged model (Fig. 2) shows clear differences in

284 densities between landscapes and within the dendritic landscape at the end of the

285 experiment (day 15).

286 The observed differences in densities follow theoretical predictions to a large extent

287 quantitatively (Tab. 1, Fig. 3). Fitting the theoretical expectations summarized in Tab. 1

288 to the density data of day 15 allowed us to estimate dispersal rates (*d*) and carrying

289 capacities (*K*) as well as compare data and model expectations. While fitting the

290 expected densities of Tab. 1 to data from linear and dendritic landscapes assuming

291 identical dispersal rates and carrying capacities across networks recaptured the

292 empirical patterns qualitatively, fitting the expectations for linear and dendritic

293 landscapes assuming network specific *d* and *K* values separately yielded a better fit

294 between data and expectations regardless of the higher number of parameters (ΔAICc =

295 12.97; Fig. 3). While the joint fitting yielded an estimate of *d* = 0.30 ($\pm$ 0.14) and of *K* =

296 3589 ($\pm$ 346; estimate $\pm$ std. error), the landscape specific fits estimate higher dispersal

297 rates and carrying capacities in the dendritic compared to the linear landscapes: $d_{dendritic}$

298 = 0.25 ($\pm$0.10), $K_{dendritic}$ = 4896 ($\pm$ 429), d_{linear} = 0.0005 ($\pm$ 0.59), K_{linear} = 2282 ($\pm$429).

299 Besides predicting a specific spatial distribution of densities in the different networks,

300 our simplified theoretical expectations (Tab. 1) as well as current theoretical work

301 (Fronhofer & Altermatt, 2017) predict higher variation in population densities within

13

302   dendritic networks compared to linear landscapes. Our experimental data support these

303   model predictions, as a conservative measure of variation (the interquartile range, IQR)

304   standardized with the median of population densities showed a non-random deviation

305   towards larger values in dendritic compared to linear landscapes (Fig. 4).

306   While we did not find differences in movement between patches or landscapes (Fig. 5,

307   Tab. 3), we did find an overall positive density dependence of movement (Fig. 6, Tab.

308   4).

309

310   **Discussion**

311   We experimentally demonstrated that differing network configurations, specifically

312   dendritic *vs.* linear networks, can result in different spatial density distributions of

313   single-species populations in otherwise completely homogeneous environments (Figs. 1

314   to 4) both across these networks (dendritic *vs.* linear) as well as within these networks

315   (central *vs.* outer *vs.* inner nodes). Thereby, the dendritic network structure and

316   dispersal therein have a direct effect on the population dynamics and structure of the

317   spatially structured population (metapopulation *sensu lato*). This ecological

318   consequence of dispersal in differently structured networks, that is, the dependence of

319   density on network position and connectivity, is the precondition for subsequent

320   evolutionary dynamics predicted to occur in networks of differing connectivity

321   (Henriques-Silva *et al.*, 2015; Fronhofer & Altermatt, 2017). Remarkably, we observe

322   these differences despite (weakly) density-dependent movement (Fig. 6), which is

323   supposed to homogenize population densities across a landscape.

324   The effect of network structure on community dynamics and occurrence of

325   organisms has been extensively studied, with a strong recent focus on particular

326   network types, such as dendritic riverine networks (e.g., Grant, Lowe & Fagan, 2007;

327 Muneepeerakul *et al.*, 2008; Carrara *et al.*, 2012; Peterson *et al.*, 2013; Mari *et al.*,

328 2014; Seymour, Fronhofer & Altermatt, 2015). In all of these studies, the occurrence

329 of organisms in individual patches/nodes within the network has been linked to

330 network position, and a dependency of genetic structure and evolutionary dynamics due

331 to network structure has been theoretically predicted (e.g., Labonne *et al.*, 2008;

332 Henriques-Silva *et al.*, 2015; Paz-Vinas & Blanchet, 2015; Paz-Vinas *et al.*, 2015;

333 Fronhofer & Altermatt, 2017). While these studies include population dynamics, which

334 subsequently affect extinction risks (Fagan, 2002; Fronhofer & Altermatt, 2017), the

335 direct effect of network connectivity and network topology on population dynamics has

336 been largely ignored experimentally. To our knowledge, our study is the first

337 experimental demonstration of a direct effect of network structure and position on

338 population densities. Specifically, we find more variable population densities in

339 dendritic compared to linear networks (Fig. 4), with inner nodes of these dendritic

340 networks exhibiting increased population sizes (Figs. 1 & 2) as predicted by theory

341 (Tab. 1 and Fig. 3). Our landscapes were of identical overall environmental conditions,

342 and local patches only differed in their connectivity. Thus, the difference in population

343 densities is a direct and inherent consequence of active dispersal across different

344 connectivity driving ecological population dynamics of our study organism

345 *Tetrahymena*.

346   Although all patches had the same initial resource availability, subsequent

347 decreases in resources due to consumption by bacteria and protists, may lead to

348 emergent variation in resource availability. While we do observe a general decrease of

349 population densities over time (Fig. 2, Tab. 2; likely as a consequence of resource

350 depletion), importantly, the difference in population densities we observed is still

351 ultimately driven by the different network configuration.

352   Interestingly, our results suggest that dispersal rates and carrying capacities

353   differ at the end of the experiment in dendritic *vs*. linear networks (Fig. 3). Most likely

354   only overall densities differ, as the errors of the dispersal rate estimates are rather large

355   and clearly overlap. Our movement data also suggest no differences in movement

356   between landscapes (Fig. 5, Tab. 2). We can only speculate about the underlying

357   mechanisms, but one possibility would be weak density regulation above K (convex

358   population regulation function). Our theoretical predictions only consider one time

359   step, respectively that density regulation always resets population sizes to K. If this is

360   not the case, differences in densities could potentially accumulate over time and lead to

361   an increase in population densities.

362   The ecological and evolutionary consequences of the observed effect of

363   connectivity on density are manifold. First, these observed differences in densities are

364   the basis of subsequent evolutionary changes, such as evolutionary differences in

365   dispersal rates in networks of different connectivities (Henriques-Silva *et al.*, 2015;

366   Fronhofer & Altermatt, 2017). These evolutionary differences may even feed back on

367   the ecological dynamics of the entire spatially structured population and alter

368   metapopulation dynamics (Fronhofer & Altermatt, 2017). Second, our single-species

369   metapopulation study also shows an underlying mechanism of the observed lower

370   species richness values in isolated headwaters both in real river networks (e.g.,

371   Altermatt, Seymour & Martinez, 2013; Liu *et al.*, 2013; Heino *et al.*, 2015; but see

372   Besemer *et al.*, 2013) as well as in experimental river-like networks (Carrara *et al.*,

373   2012; Carrara *et al.*, 2014; Seymour & Altermatt, 2014; Seymour, Fronhofer &

374   Altermatt, 2015): the lower connectivity and thus reduced immigration have direct

375   negative effects on local population densities, which eventually makes these

376   populations more prone to extinction purely based on demographic stochasticity.

377   Our findings from a single-species metapopulation model system are also

378   informative for multi-species metacommunities and the observed direct effect of

379   network structure and position on population densities has important implications for

380   the coexistence of multiple species. For example, the increased population densities in

381   inner nodes of dendritic networks will reduce local population extinctions due to drift,

382   and can thus be an underlying cause of a larger number of coexisting species at these

383   nodes in dendritic metacommunities. However, this scenario assumes that species are

384   not directly competing for the same resources and that densities of multiple species are

385   not negatively correlated with each other. In the case of direct competition, the effect of

386   dispersal and network position on higher local population persistence may be

387   counteracted by increased competition of multiple species for the same resources. Thus,

388   while we show for a single species how dispersal and network position affects

389   population sizes, the subsequent community consequences will depend on the interplay

390   between drift, species-specific dispersal and competition between the species (Vellend,

391   2010). Furthermore, dynamics in multi-species metacommunities will also be affected

392   by a higher biological heterogeneity, as different species have different dispersal rates

393   and dispersal distances, and may differently adjust their dispersal with respect to intra-

394   and interspecific densities (Fronhofer, Kropf & Altermatt, 2015; Fronhofer *et al.*,

395   2015; Cote *et al.*, 2017).

396   In our experiments we also observed a dependency of movement (as a proxy of

397   dispersal) on population density (Fig. 6, Tab. 4) as in previous studies (Pennekamp *et*

398   *al.*, 2014; Fronhofer, Kropf & Altermatt, 2015). However, this effect was rather weak,

399   as we did not find it space (Fig. 5, Tab. 3). It is remarkable that we find the expected

400   differences in population densities despite density-dependent movement, as density-

401   dependent movement is supposed to homogenize densities across space. This

402   underlines the strength of the effect of network structure on generating heterogeneity in

403   population densities.

404   Our microcosm experiments were not designed to mimic a natural system in

405   detail, but rather to test the significance of network structure in a causal way.

406   Nevertheless, the observed patterns may guide our understanding of population

407   dynamics in real river systems, as the studied network topologies can be seen as simple

408   but realistic descriptions of real river networks (Altermatt, 2013). For example, it is a

409   common phenomenon to find strong temporal but also spatial dynamics in population

410   densities for many types of organisms in riverine ecosystems. These dynamics may also

411   seen in classic "bloom" phenomena of mass-emergences of certain aquatic

412   invertebrates (e.g., mayflies) that can be found in some riverine ecosystems. In the past,

413   many of these spatio-temporal dynamics have been linked to local environmental

414   conditions (for two recent examples, e.g., Heino et al., 2015; Kaelin & Altermatt,

415   2016). Our work shows that the specific position within a river network, and the

416   dependency of local population dynamics shaped by spatially explicit topologies of

417   neighboring populations may be an additional mechanism generating variation in

418   population abundances. Thus, tributaries may enhance the abundance of organisms at

419   confluences and, as previously documented, also richness (Fernandes, Podos &

420   Lundberg, 2004). As a consequence, fluctuations in population abundances due to the

421   spatial position and connectivity of the respective population in the river network may

422   be affecting species interactions and community dynamics, and influence higher level

423   diversity metrics and metacommunity dynamics. Thus, our findings identify network

424   topology as a possible additional mechanisms generating dynamics in population and

425   community fluctuations in riverine organisms. The experimentally observed patterns

426   are not only matching empirically observed patterns in real systems (Morrissey & de

427   Kerckhove, 2009; Grant, Lowe & Fagan, 2007), but are also substantiating theoretical

428   predictions. We thus think that the patterns are robust and of general significance. Our

429   results highlight the importance of taking into account the explicit spatial structure of

430   metapopulations and metacommunities for understanding population dynamics and

431   dispersal strategies. While these findings do not preclude the significance of other

432   environmental drivers on both the occurrence as well as the abundance of organisms in

433   riverine networks, they indicate that some of the observed patterns, or at least some of

434   the unexplained variation therein, may be driven by inherent characteristics of the

435   dendritic networks themselves.

436

437   **Acknowledgements**

441

442   **Author contributions**

443   FA and EAF planned the experiment; EAF performed the experiment and analysed the

444   data; FA wrote the manuscript and EAF contributed to revisions.

445

446   **References**

447   Altermatt F. (2013) Diversity in riverine metacommunities: a network perspective

448   *Aquatic Ecology,* **47,** 365-377.

449   Altermatt F., Fronhofer E.A., Garnier A., Giometto A., Hammes F., Klecka J., Legrand

450   D., Mächler E., Massie T.M., Pennekamp F., Plebani M., Pontarp M.,

451   Schtickzelle N., Thuillier V. & Petchey O.L. (2015) Big answers from small

452   worlds: a user's guide for protist microcosms as a model system in ecology and

453   evolution. *Methods in Ecology and Evolution,* **6,** 218-231.

454   Altermatt F., Seymour M. & Martinez N. (2013) River network properties shape α-

455   diversity and community similarity patterns of aquatic insect communities

456   across major drainage basins. *Journal of Biogeography,* **40,** 2249-2260.

457   Bell G. & Gonzalez A. (2009) Evolutionary rescue can prevent extinction following

458   environmental change. *Ecology Letters,* **12,** 942-948.

459   Besemer K., Singer G., Quince C., Bertuzzo E., Sloan W. & Battin T.J. (2013)

460   Headwaters are critical reservoirs of microbial diversity for fluvial networks.

461   *Proceeding of the Royal Society B-Biological Sciences,* **280,** 1760-1760.

462   Bonte D., Van Dyck H., Bullock J.M., Coulon A., Delgado M., Gibbs M., Lehouck V.,

463   Matthysen E., Mustin K. & Saastamoinen M. (2012) Costs of dispersal.

464   *Biological Reviews,* **87,** 290-312.

465   Brown B.L. & Swan C.M. (2010) Dendritic network structure constrains

466   metacommunity properties in riverine ecosystems. *Journal of Animal Ecology,*

467   **79,** 571-580.

468   Cadotte M.W., Mai D.V., Jantz S., Collins M.D., Keele M. & Drake J.A. (2006) On

469   Testing the Competition-Colonization Trade-Off in a Multispecies Assemblage.

470   *The American Naturalist,* **168,** 704-709.

471   Carrara F., Altermatt F., Rodriguez-Iturbe I. & Rinaldo A. (2012) Dendritic

472   connectivity controls biodiversity patterns in experimental metacommunities.

473   *Proceedings of the National Academy of Sciences,* **109,** 5761-5766.

474   Carrara F., Giometto A., Seymour M., Rinaldo A. & Altermatt F. (2015) Experimental

475   evidence for strong stabilizing forces at high functional diversity in aquatic

476   microbial communities. *Ecology,* **96,** 1340-1350.

477   Carrara F., Rinaldo A., Giometto A. & Altermatt F. (2014) Complex interaction of

478   dendritic connectivity and hierarchical patch size on biodiversity in river-like

479   landscapes. *American Naturalist,* **183,** 13-25.

480   Cote J., Bestion E., Jacob S., Travis J., Legrand D. & Baguette M. (2017) Evolution of

481   dispersal strategies and dispersal syndromes in fragmented landscapes.

482   *Ecography*, **40,** 56-73.

483   Dudgeon D., Arthington A.H., Gessner M.O., Kawabata Z.I., Knowler D.J., Lévêque

484   C., Naiman R.J., Prieur-Richard A.H., Soto D., Stiassny M.L.J. & Sullivan C.A.

485   (2006) Freshwater biodiversity: importance, threats, status and conservation

486   challenges. *Biological Reviews,* **81,** 163-182.

487   Fagan W.F. (2002) Connectivity, fragmentation, and extinction risk in dendritic

488   metapopulations. *Ecology,* **83,** 3243-3249.

489   Fagan W.F., Grant E.H.C., Lynch H.J. & Unmack P. (2009) Riverine landscapes:

490   ecology for an alternative geometry. In: *Spatial Ecology.* (Eds R.S. Cantrell &

491   C. Cosner & S. Ruan). Chapman Hall Press, Boca Raton.

492   Fernandes C. C., J. Podos & J. G. Lundberg (2004) Amazonian ecology: Tributaries

493   enhance the diversity of electric fishes. *Science,* **305,** 1960-1962.

494   Fjerdingstad E., Schtickzelle N., Manhes P., Gutierrez A. & Clobert J. (2007)

495   Evolution of dispersal and life history strategies - *Tetrahymena* ciliates. *BMC

496   Evolutionary Biology,* **7,** 133.

497   Fronhofer E.A. & Altermatt F. (2015) Eco-evolutionary dynamics during experimental

498   range expansions. *Nature Communications,* **6,** 6844.

499   Fronhofer E.A. & Altermatt F. (2017) Classical metapopulation dynamics and eco-

500   evolutionary feedbacks in dendritic networks. *Ecography,* **in press**.

501   Fronhofer E.A., Klecka J., Melian C.J. & Altermatt F. (2015) Condition-dependent

502   movement and dispersal in experimental metacommunities. *Ecology Letters,* **18,**

503   954-963.

504   Fronhofer E.A., Kropf T. & Altermatt F. (2015) Density-dependent movement and the

505   consequences of the Allee effect in the model organism *Tetrahymena*. *Journal*

506   *of Animal Ecology,* **84,** 712-722.

507   Fronhofer E.A., Nitsche N. & Altermatt F. (2017) Information use shapes the dynamics

508   of range expansions into environmental gradients. *Global Ecology and*

509   *Biogeography,* **26,** 400-411.

510   Gause G.F. (1934) *The Struggle for Existence,* Dover Publications, Mineaola, N.Y.

511   Giometto A., Altermatt F., Carrara F., Maritan A. & Rinaldo A. (2013) Scaling body

512   size fluctuations. *Proceedings of the National Academy of Sciences,* **110,** 4646-

513   4650.

514   Giometto A., Rinaldo A., Carrara F. & Altermatt F. (2014) Emerging predictable

515   features of replicated biological invasion fronts. *Proceedings of the National*

516   *Academy of Sciences,* **111,** 297-301.

517   Giometto A., Altermatt F. & Rinaldo A. (2017). Demographic stochasticity and

518   resource autocorrelation control biological invasions in heterogeneous

519   landscapes. *Oikos,* In press.

520   Grant E.H.C., Lowe W.H. & Fagan W.F. (2007) Living in the branches: population

521   dynamics and ecological processes in dendritic networks. *Ecology Letters,* **10,**

522   165-175.

523   Hanski I. (1999) *Metapopulation ecology,* Oxford University Press, Oxford.

524   Heino J., Melo A.S., Bini L.M., Altermatt F., Al-Shami S.A., Angeler D.G., Bonada N.,

525   Brand C., Callisto M., Cottenie K., Dangles O., Dudgeon D., Encalada A.,

526   Göthe E., Grönroos M., Hamada N., Jacobsen D., Landeiro V.L., Ligeiro R.,

527   Martins R.T., Miserendino M.L., Md Rawi C.S., Rodrigues M.E., Roque

528   F.D.O., Sandin L., Schmera D., Sgarbi L.F., Simaika J.P., Siqueira T.,

529   Thompson R.M. & Townsend C.R. (2015) A comparative analysis reveals weak

530   relationships between ecological factors and beta diversity of stream insect

531   metacommunities at two spatial levels. *Ecology and Evolution,* **5,** 1235-1248.

532   Heino J., Muotka T. & Paavola R. (2003) Determinants of Macroinvertebrate Diversity

533   in Headwater Streams: Regional and Local Influences. *Journal of Animal*

534   *Ecology,* **72,** 425-434.

535   Henriques-Silva R., Boivin F., Calcagno V., Urban M.C. & Peres-Neto P.R. (2015) On

536   the evolution of dispersal via heterogeneity in spatial connectivity. *Proceedings*

537   *of the Royal Society B: Biological Sciences,* **282**.

538   Hiltunen T., Ayan G.B. & Becks L. (2015) Environmental fluctuations restrict eco-

539   evolutionary dynamics in predator–prey system. *Proceedings of the Royal*

540   *Society B: Biological Sciences,* **282**.

541   Hiltunen T. & Becks L. (2014) Consumer co-evolution as an important component of

542   the eco-evolutionary feedback. *Nature Communications,* **5,** 5226.

543   Holyoak M. & Lawler S.P. (1996) Persistence of an extinction-prone predator-prey

544   interaction through metapopulation dynamics. *Ecology,* **77,** 1867-1879.

545   Jacob S., Chaine A.S., Schtickzelle N., Huet M. & Clobert J. (2015) Social information

546   from immigrants: multiple immigrant-based sources of information for dispersal

547   decisions in a ciliate. *Journal of Animal Ecology,* **84,** 1373-1383.

548   Jessup C.M., Kassen R., Forde S.E., Kerr B., Buckling A., Rainey P.B. & Bohannan

549   B.J.M. (2004) Big questions, small worlds: microbial model systems in ecology.

550   *Trends in Ecology & Evolution,* **19,** 189-197.

551   Kaelin K. & F. Altermatt (2016) Landscape-level predictions of diversity in river

552   networks reveal opposing patterns for different groups of macroinvertebrates.

553   *Aquatic Ecology,* **50,** 283-295.

554   Labonne J., Ravigné V., Parisi B. & Gaucherel C. (2008) Linking dendritic network

555   structures to population demogenetics: The downside of connectivity. *Oikos,*

556   **117,** 1479-1490.

557   Leibold M.A., Holyoak M., Mouquet N., Amarasekare P., Chase J.M., Hoopes M.F.,

558   Holt R.D., Shurin J.B., Law R., Tilman D., Loreau M. & Gonzalez A. (2004)

559   The metacommunity concept: a framework for multi-scale community ecology.

560   *Ecology Letters,* **7,** 601-613.

561   Liu J., Soininen J., Han B.-P. & Declerck S.a.J. (2013) Effects of connectivity,

562   dispersal directionality and functional traits on the metacommunity structure of

563   river benthic diatoms. *Journal of Biogeography,* **40,** 2238-2248.

564   Livingston G., Matias M., Calcagno V., Barbera C., Combe M., Leibold M.A. &

565   Mouquet N. (2012) Competition-colonization dynamics in experimental

566   bacterial metacommunities. *Nature Communications,* **3**.

567   Lynch H.J., Grant E.H.C., Muneepeerakul R., Arunachalam M., Rodriguez-Iturbe I. &

568   Fagan W.F. (2011) How restructuring river connectivity changes freshwater fish

569   biodiversity and biogeography. *Water Resources Research,* **47,** W05531.

570   Mari L., Casagrandi R., Bertuzzo E., Rinaldo A. & Gatto M. (2014) Metapopulation

571   persistence and species spread in river networks. *Ecology Letters,* **14,** 426-434.

572   Morrissey M.B. & De Kerckhove D.T. (2009) The maintenance of genetic variation

573   due to asymmetric gene flow in dendritic metapopulations. *The American*

574   *Naturalist,* **174,** 875-889.

575   Muneepeerakul R., Bertuzzo E., Lynch H.J., Fagan W.F., Rinaldo A. & Rodriguez-

576   Iturbe I. (2008) Neutral metacommunity models predict fish diversity patterns

577   in Mississippi-Missouri basin. *Nature,* **453,** 220-222.

578   Paz-Vinas I. & Blanchet S. (2015) Dendritic connectivity shapes spatial patterns of

579   genetic diversity: a simulation-based study. *Journal of Evolutionary Biology,*

580   **28,** 986-994.

581   Paz-Vinas I., Loot G., Stevens V.M. & Blanchet S. (2015) Evolutionary processes

582   driving spatial patterns of intraspecific genetic diversity in river ecosystems.

583   *Molecular Ecology,* **24,** 4586-4604.

584   Pennekamp F., Mitchell K.A., Chaine A. & Schtickzelle N. (2014) Dispersal propensity

585   in *Tetrahymena thermophila* ciliates—a reaction norm perspective. *Evolution,*

586   **68,** 2319-2330.

587   Pennekamp F. & Schtickzelle N. (2013) Implementing image analysis in laboratory-

588   based experimental systems for ecology and evolution: a hands-on guide.

589   *Methods in Ecology and Evolution,* **4,** 483-492.

590   Peterson E.E., Ver Hoef J.M., Isaak D.J., Falke J.A., Fortin M.-J., Jordan C.E., Mcnyset

591   K., Monestiez P., Ruesch A.S., Sengupta A., Som N., Steel E.A., Theobald

592   D.M., Torgersen C.E. & Wenger S.J. (2013) Modelling dendritic ecological

593   networks in space: an integrated network perspective. *Ecology Letters,* **16,** 707-

594   719.

595   Pinheiro J., Bates D.M., S. D., Sarkar D., Eispack Authors, Heisterkamp S. & Van

596   Willigen B. (2016) nlme: Linear and Nonlinear Mixed Effects Models. (Ed R.-

597   C. Project). R-core Team.

598   R Development Core Team. (2016) R: A language and environment for statistical

599   computing. Version 3.3.2. R Foundation for Statistical Computing, Vienna,

600   Austria.

601   Rodriguez-Iturbe I. & Rinaldo A. (1997) *Fractal river networks: chance and self-*

602   *organization,* Cambridge University Press, New York.

603   Seymour M. & Altermatt F. (2014) Active colonization dynamics and diversity patterns

604   are influenced by dendritic network connectivity and species interactions.

605   *Ecology and Evolution,* **4,** 1243-1254.

606   Seymour M., Fronhofer E.A. & Altermatt F. (2015) Dendritic network structure and

607   dispersal affect temporal dynamics of diversity and species persistence. *Oikos,*

608   **124,** 908-916.

609   Tonkin J.D. (2014) Drivers of macroinvertebrate community structure in unmodified

610   streams. *PeerJ,* **2,** e465.

611   Van Petegem K.H.P., Boeye J., Stoks R. & Bonte D. (2016) Spatial selection and local

612   adaptation jointly shape life-history evolution during range expansion.

613   *American Naturalist,* **188,** 485-495.

614   Vellend M. (2010) Conceptual synthesis in community ecology. *The Quarterly Review*

615   *of Biology,* **85,** 183-207.

616   Vorosmarty C.J., Mcintyre P.B., Gessner M.O., Dudgeon D., Prusevich A., Green P.,

617   Glidden S., Bunn S.E., Sullivan C.A., Liermann C.R. & Davies P.M. (2010)

618   Global threats to human water security and river biodiversity. *Nature,* **467,** 555-

619   561.

620

621

622   **Tables**

623   Table 1: Theoretical expectation of the distribution of densities in dendritic and linear

624   networks (Fig. 1) based solely on the assumption of active dispersal and the network`s

625   connectivity pattern. Initially, patches are assumed to have K individuals. Patches lose

626   all their emigrants ($d\,K$; d being the dispersal rate), which are distributed equally to

627   connecting patches. Patches will receive a fraction of the emigrants from connecting

628   patches. For example, due to an edge effect, an outer patch in a dendritic landscape will

629   loose $d\,K$ emigrants and only receive $\frac{1}{3}d\,K$ immigrants from a connecting inner patch,

630   as inner patches distribute their emigrants over 3 vertices. Note that we here neglect the

631   effect of dispersal mortality (Bonte *et al.*, 2012), as dispersal related mortality is likely

632   very low in our experimental systems.

633

	Linear	Dendritic
Outer	$\left(1-\frac{1}{2}d\right)K$	$\left(1-\frac{2}{3}d\right)K$
Inner	$\left(1+\frac{1}{2}d\right)K$	$\left(1+\frac{4}{3}d\right)K$
Central	K	K

634

635

636   Table 2. Linear mixed model selection and averaging based on ΔAICc and AICc

637   weights (W_{AICc}) for square-root transformed density data and models fitted using

638   maximum likelihood (see Fig. 2 for a visualization). "Time" is a continuous variable

639   and includes measurements on day 0, 8 and 15; "position" is a factor capturing whether

640   densities were measured in central, inner or outer patches (see Fig. 1) ; "network" is a

641   factor capturing whether densities were measured in linear or dendritic landscapes. The

642   random effect structure is "time" nested in "landscape ID". Model components and

643   corresponding codes are: time (1), network (2), position (3), time:network (4),

644   time:position (5), network:position (6), time:network:position (7).

Model components	df	ΔAICc	W_{AICc}
1, 2, 3, 4, 5, 6, 7	16	0	0.44
1, 2, 3, 4, 6	12	0.78	0.30
1, 2, 3, 4, 5, 6	14	2.40	0.13
1, 2, 3, 6	11	3.54	0.07
1, 2, 3, 5, 6	13	4.92	0.04
2, 3, 6	10	7.05	0.01
1, 2, 3, 4	10	9.28	0
1, 2, 3, 4, 5	12	10.78	0
1, 2, 3	9	12.08	0
1, 2, 3, 5	11	13.36	0
2, 3	8	15.65	0
1, 2, 4	8	15.90	0
1, 2	7	18.76	0
1, 3	8	22.19	0
2	6	22.38	0

1, 3, 5	10	23.53	0
3	7	25.68	0
1	6	28.45	0
null model	5	32.00	0

645
646

1, 3, 5	10	23.53	

647   Table 3. Linear mixed model selection and averaging based on ΔAICc and AICc

648   weights (W_{AICc}) for log transformed movement data (Euclidean distance moved) and

649   model fitted using maximum likelihood (for a visualization see Fig. 5). "Time" is a

650   continuous variable and includes measurements on day 0, 8 and 15; "position" is a

651   factor capturing whether movement was measured in central, inner or outer patches

652   (see Fig. 1); "network" is a factor capturing whether movement was measured in linear

653   or dendritic landscapes. The random effect structure is "time" nested in "landscape ID".

654   Model components and corresponding codes are: time (1), network (2), position (3),

655   time:network (4), time:position (5), network:position (6), time:network:position (7).

Model components	df	ΔAICc	W_{AICc}
1	6	0	0.96
1, 2	7	7	0.03
1, 3	8	9.45	0.01
1, 2 , 3	9	16.80	0
1, 2, 4	8	17.16	0
null model	5	18.82	0
1, 2, 3, 6	11	19.26	0
2	6	24.24	0
1, 2, 3, 4	10	26.97	0
3	7	27.53	0
1, 3, 5	10	28.67	0
1, 2, 3, 4, 6	12	29.06	0
2, 3	8	33.99	0
1, 2, 3, 5	11	35.71	0
2, 3, 6	10	36.15	0
1, 2, 3, 5, 6	13	38.09	0

1, 2, 3, 4, 5	12	46.78	0
1, 2, 3, 4, 5, 6	14	49.11	0
1, 2, 3, 4, 5, 6, 7	16	68.29	0

656

1, 2, 3, 4, 5	12	46.78	0

657   Table 4. Linear mixed model selection and averaging based on ΔAICc and AICc

658   weights (W_{AICc}) for log transformed movement data (Euclidean distance moved) as a

659   function of density. Models were fitted using maximum likelihood (for a visualization

660   see Fig. 6). "network" is a factor capturing whether movement was measured in linear

661   or dendritic landscapes. "Density" is a continuous variable capturing the local

662   population density in which movement was measured. The random effect structure is

663   "time" nested in "network" and "position" (central, inner, outer; see Fig. 1). Model

664   components and corresponding codes are: density (1), network (2), squared density (3),

665   cubed density (4), density:network (5), squared density:network (6), cubed

666   density:network (7).

Model components	df	ΔAICc	W_{AICc}
1	9	0	0.42
1, 2	10	2.07	0.15
3	10	2.19	0.14
4	11	3.34	0.08
1, 2, 5	11	3.84	0.06
2, 3	11	4.27	0.05
null model	8	4.28	0.05
2, 4	12	5.51	0.03
2	9	6.21	0.02
2, 3, 6	13	6.64	0.02
2, 4, 7	15	11.31	0

667
668
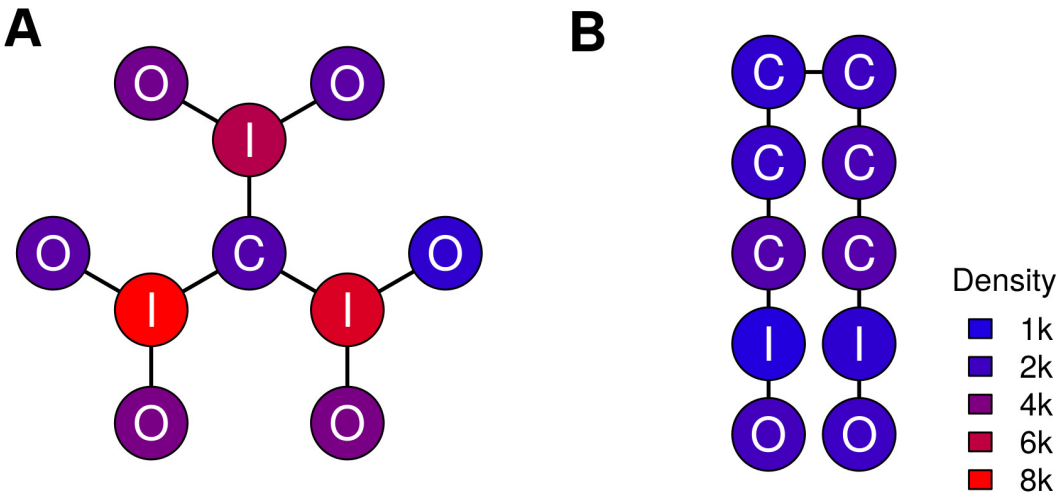
669   **Figure legends**

670

671

672   Fig. 1: Median population densities (in thousands of individuals) of *Tetrahymena* in

673   corresponding dendritic (A) and linear (B) landscapes at the end of the experiment (day

674   15) and across the three replicate landscapes. In these landscapes, outer nodes are

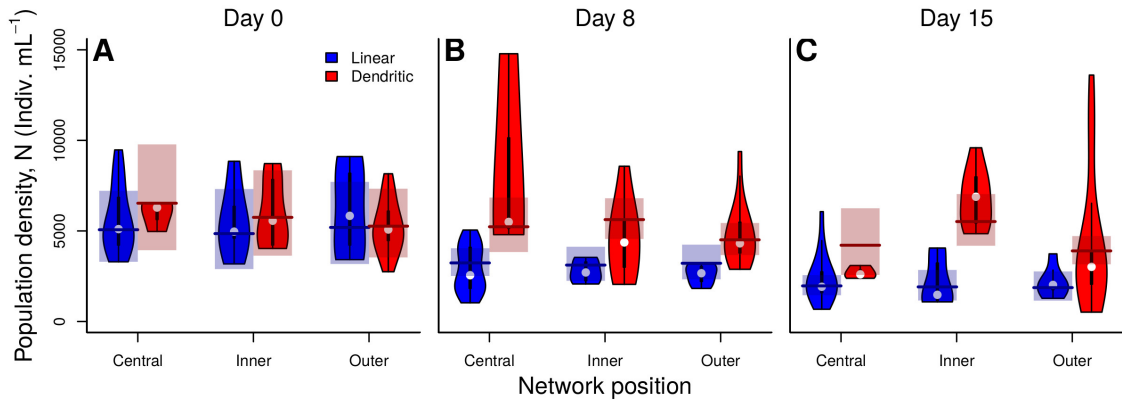675   labeled "O", inner and central nodes are labeled "I" and "C" respectively.

676

677

678

679   Fig. 2: Distribution of *Tetrahymena* population densities depending on network type

680   (linear *vs.* dendritic networks), network position (central vs. inner *vs.* outer nodes) and

681   time (days 0, 8, and 15). Violin plots show the overall distribution of the data, the white

682   point gives the median, and the solid black line the 25% and 75% percentiles

683   respectively. Given the network structure (Fig. 1) and the 3 replicates per landscape,

684   distributions include N=18 (9, 3) measurements for outer (inner, central) nodes of

685   dendritic networks and N=6 (6, 18) measurements for outer (inner, central) nodes of

686   linear landscapes. Horizontal lines visualize back-transformed parameter estimates of

687   the averaged linear mixed effects model and shaded areas show 95% confidence

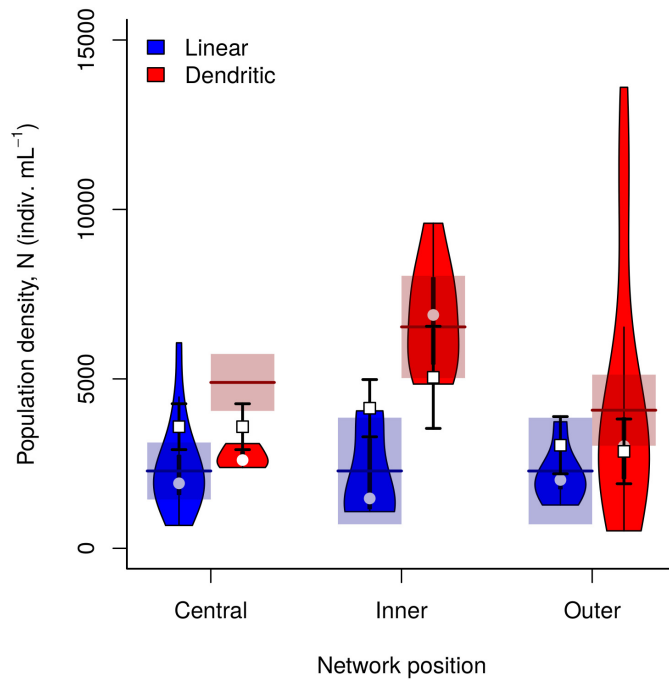688   intervals (see Tab. 1 for model selection results).

689

690

691   Fig. 3: Fit of theoretical expectations to the distribution of *Tetrahymena* population

692   densities depending on network type (linear *vs.* dendritic networks), network position

693   (central vs. inner *vs.* outer nodes) for day 15. Violin plots show the overall distribution

694   of the data, the white point gives the median, and the solid black line the 25% and 75%

695   percentiles respectively. Given the network structure (Fig. 1) and the 3 replicates per

696   landscape, distributions include N=18 (9, 3) measurements for outer (inner, central)

697   nodes of dendritic networks and N=6 (6, 18) measurements for outer (inner, central)

698   nodes of linear landscapes. Horizontal red and blue lines visualize fits of the

699   theoretically expected distribution of population densities to data from the dendritic and

700   linear networks assuming network specific dispersal rates (*d*) and carrying capacities

701   (*K*). White squares show fits of the theoretically expected distribution of population

702   densities assuming the same *d* and *K* values for both network types.

703   Shaded areas, respectively error bars, show 95% confidence intervals of the fits.
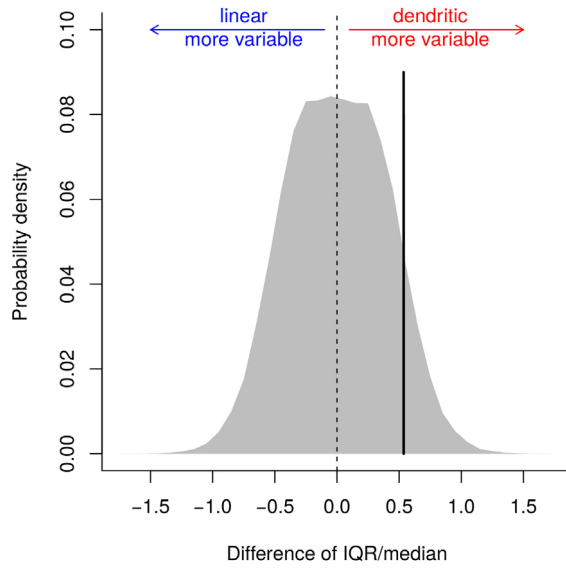
704

705

706

707   Fig. 4: Comparison of variation in population densities between linear and dendritic

708   networks at day 15 of the experiment. The solid line represents the difference between

709   inter-quartile range (IQR) over median population densities of linear and dendritic

710   landscapes. The distribution (grey) represents the distribution of the differences

711   between IQR over median population densities of 200,000 random re-samplings for our

712   data. As we theoretically expect the dendritic landscapes to be more variable we can

713   perform a one-sided test which gives a probability of p=0.047 of our observed

714   difference between IQR to median ratios to be larger than zero.
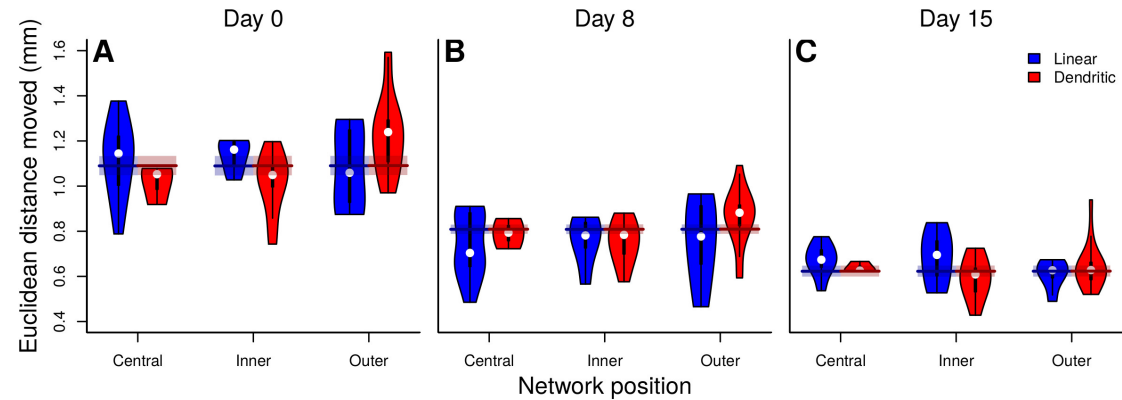
715

716

717

718   Fig. 5. Euclidean distances moved by *Tetrahymena* individuals depending on network

719   type (linear *vs.* dendritic networks), network position (central vs. inner *vs.* outer nodes)

720   and time (days 0, 8, and 15). Violin plots show the overall distribution of the data, the

721   white point gives the median, and the solid black line the 25% and 75% percentiles

722   respectively. Given the network structure (Fig. 1) and the 3 replicates per landscape

723   distributions include N=18 (9, 3) measurements for outer (inner, central) nodes of

724   dendritic networks and N=6 (6, 18) measurements for outer (inner, central) nodes of

725   linear landscapes. Horizontal lines visualize back-transformed parameter estimates of

726   the averaged linear mixed effects model and shaded areas show 95% confidence

727   intervals (see Tab. 2 for model selection results).
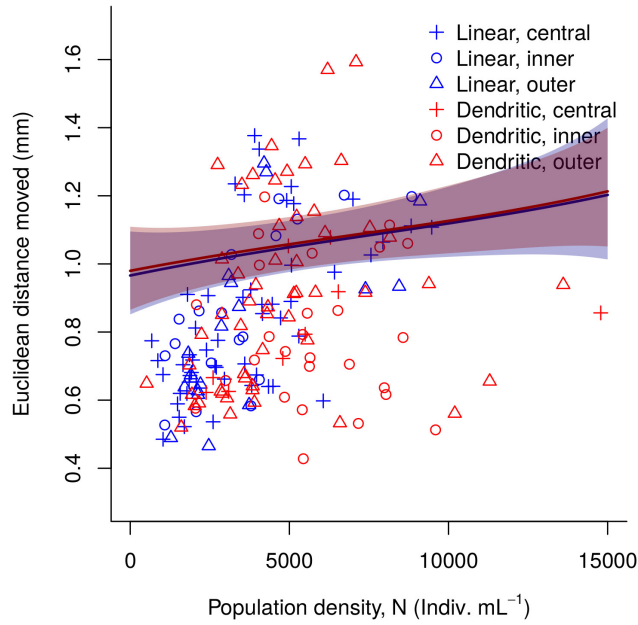
728

729
730
731　Fig. 6: Euclidean distances moved by *Tetrahymena* individuals depending on densities

732　in our entire dataset. Across all replicates of all landscapes (patches from different

733　landscapes types highlighted by different symbols; see legend) we find positively

734　density-dependent movement. The solid lines represent fits of the averaged linear

735　mixed model (red: dendritic landscapes; blue: linear landscapes) and the shaded area

736　shows 95% confidence intervals (see Tab. 3 for model selection results).

737